

Gluon fusion contribution to $W^+W^- + \text{jet}$ production

Tom Melia

Rudolf Peierls Centre for Theoretical Physics, 1 Keble Road, University of Oxford, UK

Email: t.melia1@physics.ox.ac.uk

Kirill Melnikov

Department of Physics and Astronomy, Johns Hopkins University, Baltimore, MD

21218, USA

Email: melnikov@pha.jhu.edu

Raoul Röntsch

Rudolf Peierls Centre for Theoretical Physics, 1 Keble Road, University of Oxford, UK

Email: r.rontsch1@physics.ox.ac.uk

Markus Schulze

High Energy Physics Division, Argonne National Laboratory, Argonne, IL 60439, USA

Email: markus.schulze@anl.gov

Giulia Zanderighi

Rudolf Peierls Centre for Theoretical Physics, 1 Keble Road, University of Oxford, UK

Email: g.zanderighi1@physics.ox.ac.uk

ABSTRACT: We describe the computation of the $gg \rightarrow W^+W^-g$ process that contributes to the production of two W -bosons and a jet at the CERN Large Hadron Collider (LHC). While formally of next-to-next-to-leading order (NNLO) in QCD, this process can be evaluated separately from the bulk of NNLO QCD corrections because it is finite and gauge-invariant. It is also enhanced by the large gluon flux and by selection cuts employed in the Higgs boson searches in the decay channel $H \rightarrow W^+W^-$, as was first pointed out by Binoth *et al.* in the context of $gg \rightarrow W^+W^-$ production. For cuts employed by the ATLAS collaboration, we find that the gluon fusion contribution to $pp \rightarrow W^+W^-j$ enhances the background by about ten percent and can lead to moderate distortions of kinematic distributions which are instrumental for the ongoing Higgs boson searches at the LHC. We also release a public code to compute the NLO QCD corrections to this process, in the form of an add-on to the package MCFM.

KEYWORDS: Higgs physics, QCD, Standard Model.

Contents

1. Introduction	1
2. Technical Details	3
3. Results	5
4. Conclusion	9
A. Appendix	10

1. Introduction

At the time of writing, the Large Hadron Collider (LHC) is running at a center-of-mass energy $\sqrt{s} = 8$ TeV, having completed a very successful 7 TeV run at the end of 2011. Collected data are consistent with the Standard Model Higgs boson with a mass of 124–126 GeV [1, 2]. As more data are collected in 2012, the evidence for the new particle in this mass range will, hopefully, become stronger, opening up the way for a detailed exploration of its properties.

Currently, the $m_H = 125$ GeV Higgs boson signal has the largest significance in $\gamma\gamma$ and ZZ^* final states. However, eventually, the signal should also appear in the W^+W^- final state thanks to the process $gg \rightarrow H \rightarrow W^+W^-$. In fact, understanding the properties of the new particle will require, at a minimum, the measurement of its branching fractions to as many final states as possible; therefore, measuring the branching fraction for $H \rightarrow W^+W^-$ is important. Higgs searches in the W^+W^- mode are performed by binning final states according to the number of jets produced. This is primarily done for a detailed identification of backgrounds and for designing cuts that maximize the signal-to-background ratio for each of the jet bins. For zero- and one-jet bins, the dominant backgrounds are $pp \rightarrow W^+W^-$ and $pp \rightarrow W^+W^- + \text{jet}$, respectively, while for the two-jet bin $pp \rightarrow t\bar{t}$ becomes dominant.

QCD radiative corrections are known to change both signal and background rates by significant, jet-bin-dependent amounts. Higgs production rates are known through next-to-next-to-leading order (NNLO) QCD in the zero-jet bin [3–5] and through NLO QCD in the one- [6–8] and two-jet bins [9, 10]. The production of a W -pair without reconstructed jets is known through NLO QCD [11–15] and has been implemented in publicly available programs such as MCFM [16], MC@NLO [17], and POWHEG [18]. The production of a W -pair in association with one jet was calculated through NLO QCD in Refs. [19–21]. The NLO QCD corrections to the production of a W -pair in association with two jets were computed in Refs. [22–24].

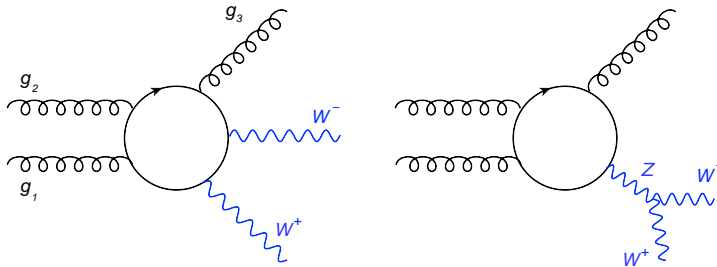


Figure 1: Sample Feynman diagrams for $gg \rightarrow W^+W^-g$ through a fermion loop.

Little is known about the main background processes beyond next-to-leading order. One exception is the study of the gluon-gluon fusion that gives rise to a pair of W -bosons through a fermion loop [25–27]. Although this contribution appears at one-loop, it cannot contribute to next-to-leading order cross-sections because there is no tree process with two gluons in the initial state. Therefore, the $gg \rightarrow W^+W^-$ sub-process is finite and a gauge-invariant part of the NNLO contribution to W^+W^- production that can be computed independently. Thanks to the low production threshold of the two W -bosons relative to the LHC center-of-mass energy, the cross-section arising from the $gg \rightarrow W^+W^-$ contribution is enhanced by the large gluon flux. To some extent, this may compensate the suppression by an additional power of α_s and lead to the numerical importance of the gluon fusion sub-process. These NNLO corrections have been studied for the production of a W -pair with no jets in Refs. [25–27]. It was found that the effect of these corrections is highly cut-dependent: for inclusive cuts they enhance the cross-section by 4–5%, which is comparable to the scale uncertainty at next-to-leading order, but the relative importance of the gluon fusion corrections increases dramatically if cuts designed to enhance the $gg \rightarrow H \rightarrow W^+W^-$ signal are applied. In fact, for the cuts of Refs. [26,27], $gg \rightarrow W^+W^-$ becomes the *dominant* radiative correction to $pp \rightarrow W^+W^-$, overshooting the NLO QCD correction to this process by a factor of around seven. The gluon induced WW production is implemented in the generators MCFM [16] and gg2WW [27]; the latter can also be interfaced to parton shower programs.

Since, as we pointed out earlier, the Higgs searches distinguish processes with different jet multiplicities and since the final state with a W -pair and a jet is an important contributor to current Higgs searches, it is a relevant question if a similar enhancement of the gluon fusion contribution occurs there as well. The goal of this paper is to study this question. To this end, we compute the gluon-induced NNLO QCD corrections to $W^+W^- + \text{jet}$ production in proton collisions and explore its numerical significance in dependence of the applied cuts.

To perform this calculation, we use a generalized unitarity implementation [28–31] of the Ossola-Pittau-Papadopoulos (OPP) procedure [32] for the reduction of tensor integrals (for a review see Ref. [31]). These on-shell techniques have had fantastic success over the past few years, leading to a large number of NLO QCD computations of very complex processes [33]. Recent developments in automating these and similar techniques for one-

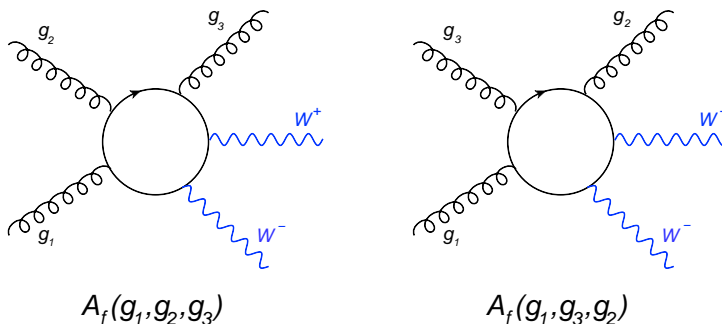


Figure 2: Primitive amplitudes $A_f(g_1, g_2, g_3)$ and $A_f(g_1, g_3, g_2)$. One ordering of the W -bosons is shown. However, we need to consider every insertion of the electroweak bosons relative to the ordered gluons.

loop computations also seem very promising [34–37].

The remainder of this paper is organized as follows. In Section 2, we provide technical details of the calculation, pointing out a few subtleties that arise when dealing with a process that involves several colorless external bosons and virtual fermions. In Section 3, we present results for typical cuts that are used to observe weak gauge boson pair production and for a different set of cuts designed to increase the significance of the Higgs boson signal. We conclude in Section 4. In the Appendix, we provide numerical results for one-loop primitive amplitudes for further comparison. Finally, we note that as a by-product of this work we release a code that allows for the NLO QCD description of the $pp \rightarrow W^+W^- + \text{jet}$ process¹. The code is in the form of a patch to the program MCFM [16], and can be obtained from <http://www-thphys.physics.ox.ac.uk/people/TomMelia/tommelia.html>, or from the MCFM website <http://mcfm.fnal.gov/>.

2. Technical Details

We consider the gluon-gluon fusion contribution to the production of a W -boson pair and a jet. At lowest order in QCD, this process occurs through a fermion loop and involves three gluons, see Fig. 1. This one-loop amplitude provides a finite, gauge-invariant contribution to the NNLO correction. We consider leptonic decays of W bosons and write the one-loop amplitude for the process $0 \rightarrow gggW^+(\rightarrow \nu_e e^+)W^-(\rightarrow \mu^- \bar{\nu}_\mu)$ as

$$\begin{aligned}
 \mathcal{A}_f^1(g_1, g_2, g_3; \nu_e, e^+, \mu^-, \bar{\nu}_\mu) &= g_s^3 \left(\frac{g_w}{\sqrt{2}} \right)^4 \times \\
 &\left(\text{Tr}(T^{a_1} T^{a_2} T^{a_3}) A_f(g_1, g_2, g_3) + \text{Tr}(T^{a_1} T^{a_3} T^{a_2}) A_f(g_1, g_3, g_2) \right).
 \end{aligned}
 \tag{2.1}$$

Here g_w and g_s are the weak and strong couplings respectively, and the A_f are color-ordered primitive amplitudes with all possible insertions of the two W bosons relative to

¹Note that the public code does not include the NLO QCD corrections coming from fermion loops – these contributions are several orders of magnitude smaller than the total cross-sections.

the ordered gluons, see Fig. 2. The normalization of the $SU(3)$ color group generators is $\text{Tr}(T^a T^b) = \delta^{ab}$. We take top and bottom quarks as massive, while the other four quarks are taken to be massless. We use a unit CKM matrix, so that each of the primitive amplitudes in Eq. (2.1) contains two massless and one massive fermion loop,

$$A_f = 2A_{f,0} + A_{f,m}. \quad (2.2)$$

It is also necessary to consider the production of WW through an intermediate Z -boson or a photon. Thus we can write the primitive amplitudes in Eq. (2.2) as

$$\begin{aligned} A_{f,0} &= A_{f,ud}^{[WW]} + \sum_{q \in \{u,d\}} \left(C_{V,q}^{[Z]} A_{f,q}^{[Z_V]} + C_{A,q}^{[Z]} A_{f,q}^{[Z_A]} + C_q^\gamma A_{f,q}^{[\gamma]} \right), \\ A_{f,m} &= A_{f,tb}^{[WW]} + \sum_{q \in \{t,b\}} \left(C_{V,q}^{[Z]} A_{f,q}^{[Z_V]} + C_{A,q}^{[Z]} A_{f,q}^{[Z_A]} + C_q^\gamma A_{f,q}^{[\gamma]} \right). \end{aligned} \quad (2.3)$$

The first term refers to the amplitudes obtained by attaching the W -bosons directly to the fermion loop. The remaining terms refer to amplitudes obtained for one flavor of quark circulating in the loop, with the W -bosons attached through the vector and axial parts of a Z -boson or a photon, respectively. The couplings are $C_{V,q}^{[Z]} = T_q^3 - 2Q_q \sin^2 \theta_w$, $C_{A,q}^{[Z]} = -T_q^3$, and $C_q^\gamma = 2Q_q \sin^2 \theta_w$, where Q_q is the electromagnetic charge of the quark in the loop, θ_w is the weak mixing angle, and $T_{u,c,t}^3 = 1/2$, $T_{d,s,b}^3 = -1/2$. For the first term in Eq. (2.3), it is necessary to consider every insertion of the W -pair relative to the ordered gluons. There are twelve such insertions, allowing for the ordering W^+W^- and W^-W^+ . Similarly, for the remaining terms, we need to account for three orderings of an intermediate Z -boson or photon relative to the gluons. We account for the decays of W -bosons $W(p_l + p_{\bar{l}}) \rightarrow l(p_l) \bar{l}(p_{\bar{l}})$ by constructing polarization vectors from lepton spinors. We write

$$\epsilon_W^\mu(p_l, p_{\bar{l}}) = \frac{-i \bar{u}(p_l) \gamma^\mu (1 - \gamma_5) v(p_{\bar{l}})}{2(s_{l\bar{l}} - m_W^2 + i\Gamma_W m_W)}, \quad (2.4)$$

where $s_{l\bar{l}} = (p_l + p_{\bar{l}})^2$ is the invariant mass of the two leptons. The definitions of the polarization vectors of the intermediate Z -boson and the photon include a large number of terms that accommodate both single and double resonant amplitudes for the production of two W -bosons. All amplitudes were checked against an independent home-made OPP-based program that can be used to compute Feynman diagrams directly. Furthermore, the term $A_{f,ud}^{[WW]}$ was checked against the publicly available program **GoSam** [34] for a few phase space points.

We compute tree level amplitudes using Berends-Giele recursion relations [38]. There is a further technical aspect to be discussed, related to the use of these recursion relations with a cyclic amplitude. To illustrate this point, we consider two orderings of the W -bosons in the primitive amplitude $A_f(g_1, g_2, g_3)$, with a different double cut on each, as shown in Fig. 3. Both of these cuts split the one-loop amplitude into two tree-level helicity amplitudes, and we focus on the one involving g_1 and W^+ . When a Berends-Giele current includes an electroweak boson, all insertions of that electroweak boson relative to the gluons are considered. In particular, this means that the tree-level amplitude arising from either

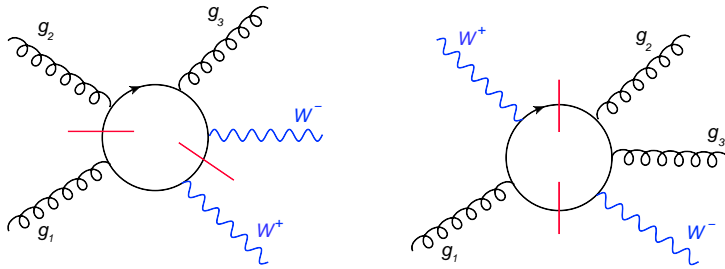


Figure 3: Two double cuts on a primitive amplitude with different orderings of the W -bosons, leading to a potential source of double counting.

cut shown will include the W^+ both before and after the gluon g_1 , reading clockwise. Since the amplitudes are cyclic, we would, in effect, be double counting. Because the cuts are on different propagators, it is difficult to identify automatically which cuts will end up duplicating one another in this manner. Instead, we observe that the cause of this problem is the cyclic nature of the amplitudes. However, looking at Eq. (2.1), it is clear that we can require gluon g_1 to be in a fixed position for both primitive amplitudes, with appropriate ordering of the other two gluons and all insertions of the W -bosons. We modify our Berends-Giele currents accordingly, so that the positions of the electroweak bosons are fixed relative to g_1 , but still allowing all insertions relative to the other two gluons. Referring again to Fig. 3, the left amplitude will have the W^+ -boson only before the gluon (again, reading clockwise), while the right amplitude will have the W^+ -boson only after the gluon, and the double counting is avoided.

3. Results

In this Section we present the results for the process $pp \rightarrow W^+W^- + \text{jet}$ at the LHC, including the gluon fusion contribution $gg \rightarrow W^+W^-g$. We consider two center-of-mass energies, $\sqrt{s} = 8$ GeV and $\sqrt{s} = 14$ TeV and let the W -bosons decay into a pair of leptons of definite flavor, $W^+W^- \rightarrow \nu_e e^+ \mu^- \bar{\nu}_\mu$. We note that the cross-section inclusive in lepton flavors $l^+l^- = \{e^+e^-, e^+\mu^-, \mu^+e^-, \mu^+\mu^-\}$ is a factor of four larger than the results presented below. We take the W -boson mass and width to be $m_W = 80.399$ GeV and $\Gamma_W = 2.085$ GeV, while the Z -boson mass and width are taken to be $m_Z = 91.1876$ GeV and $\Gamma_Z = 2.4952$ GeV. We use a top quark mass $m_t = 172.9$ GeV and a bottom quark mass $m_b = 4.19$ GeV and take all other quarks to be massless. The weak couplings are defined through the Fermi constant $G_F = 1.166364 \times 10^{-5}$ GeV $^{-2}$ with $g_w^2 = 8G_F m_W^2 / \sqrt{2}$, and the weak mixing angle is given by $\sin^2 \theta_w = 1 - m_W^2 / m_Z^2$. Jets are defined through the anti- k_\perp algorithm [39] with $R = 0.4$, as implemented in FastJet [40]. We use MSTW08 parton distribution set [41] and we employ leading, next-to-leading and next-to-next-to-leading order parton distribution functions (pdf) to compute the relevant contributions to the cross-sections. We stress that, for the purposes of this discussion, the gluon fusion process $gg \rightarrow W^+W^-g$ is a NNLO contribution and therefore it is computed with NNLO

Standard Cuts

		σ_{LO}	$\sigma_{\text{NLO}}^{\text{incl}}$	$\sigma_{\text{NLO}}^{\text{excl}}$	$\delta\sigma_{\text{NNLO}}$	$\delta\sigma_{\text{NNLO}}/\sigma_{\text{NLO}}^{\text{incl}}$
8 TeV	WW	141.0(1) $^{+2.8}_{-4.0}$	232.0(4) $^{-5.8}_{+7.5}$	143.8(2) $^{+4.2}_{-4.1}$	8.1(1) $^{-1.7}_{+2.2}$	3.5%
	WWj	87.8(1) $^{-10.9}_{+13.5}$	111.3(2) $^{-5.5}_{+4.9}$	66.6(2) $^{+4.4}_{-9.0}$	3.4(1) $^{-1.0}_{+1.6}$	3.1%
14 TeV	WW	259.6(2) $^{+14.2}_{-17.2}$	448.3(5) $^{-7.4}_{+11.6}$	242.0(3) $^{+9.2}_{-8.6}$	23.6(1) $^{-4.1}_{+5.2}$	5.3%
	WWj	203.4(1) $^{-19.9}_{+22.9}$	254.5(4) $^{-10.2}_{+9.0}$	127.6(4) $^{+14.8}_{-24.1}$	11.8(4) $^{-3.2}_{+4.7}$	4.6%

Table 1: Cross-sections for $pp \rightarrow W^+(\nu_e e^+)W^-(\mu^- \bar{\nu}_\mu) + n$ jets, $n = 0, 1$ at the $\sqrt{s} = 8$ TeV and $\sqrt{s} = 14$ TeV LHC, using the standard cuts described in the text. All cross-section values are in femtobarns. The central values are computed with factorization and renormalization scales $\mu = 2m_W$, with the statistical error shown in parentheses. The upper and lower values for cross-sections are obtained with the choice of scale $\mu = m_W$ (subscript) and $\mu = 4m_W$ (superscript). The last column shows the relative size of the NNLO contribution and the *inclusive* NLO cross-section for the central scale choice.

pdfs².

We first consider cuts that are typical for processes with W -bosons and jets, and refer to them as “standard cuts”. We require that *i*) both leptons have transverse momenta $p_{T,l} > 20$ GeV and pseudorapidity $|\eta_l| < 2.5$, *ii*) the missing transverse momentum satisfies $p_{T,\text{miss}} > 30$ GeV and *iii*) jets have transverse momenta $p_{T,j} > 20$ GeV and pseudorapidity $|\eta_j| < 3.2$. In Table 1, we show the LO and NLO cross-sections for $pp \rightarrow W^+W^- + \text{jet}$, as well as the gluon fusion (NNLO) contribution, using these cuts for two LHC energies. Also shown are the sizes of the NNLO corrections relative to the inclusive NLO cross-sections. We set the factorization and renormalization scales equal to one another, $\mu_F = \mu_R = \mu$, and show the scale variation $m_W \leq \mu \leq 4m_W$ with a central scale choice $\mu = 2m_W$. We also show the cross-sections for $pp \rightarrow W^+W^-$ without jets in Table 1, for comparison with the earlier calculation of Ref. [26]. Although the setup here is slightly different, in particular cuts on missing transverse energy, parton distribution functions and some input parameters, our results are similar to the ones reported in Ref. [26] for LO, NLO and the gluon fusion contributions to $pp \rightarrow W^+W^-$ process. It follows from Table 1 that the gluon fusion corrections are modest; they change the NLO cross-sections by 3–5% which is to be compared with $\mathcal{O}(65 - 70\%)$ inclusive NLO QCD corrections in the case of $pp \rightarrow W^+W^-$ and $\mathcal{O}(15 - 25\%)$ in the case of $pp \rightarrow W^+W^- + \text{jet}$. The relative importance of the gluon fusion contribution grows with the energy which is to be expected because of the rapid growth of the gluon flux at small values of $x \sim m_{W+W^-}/\sqrt{s}$. For both processes, $pp \rightarrow W^+W^-$ and $pp \rightarrow W^+W^- + j$, the gluon fusion corrections are comparable to the scale uncertainty of the NLO cross-section at $\sqrt{s} = 8$ TeV and slightly exceed it at $\sqrt{s} = 14$ TeV.

Next, we consider cuts similar to those used by the ATLAS collaboration in their

²We note that the use of NNLO pdfs for the computation of the gluon fusion contribution leads to a smaller result (by roughly 30%) compared to that obtained using LO pdfs, since the NNLO gluon flux is smaller than the LO flux. We nevertheless use NNLO pdfs since this is what would be done once the NNLO description of the W^+W^- production becomes available.

Higgs search in the W^+W^- channel [42] (“Higgs search cuts”). To this end, we require that *i*) the hardest lepton has $p_{T,l,\max} > 25$ GeV, the softest lepton has $p_{T,l,\min} > 15$ GeV, *ii*) the lepton rapidities are $|\eta_l| < 2.5$ ³; *iii*) the relative azimuthal angle between the two leptons is small $\Delta\phi_{ll} < 1.8$, *iv*) the two leptons are separated from each other by $\Delta R_{ll} = \sqrt{\Delta\phi_{ll}^2 + \Delta\eta_{ll}^2} > 0.3$, *v*) the invariant mass of the charged lepton system must satisfy $10 \text{ GeV} < m_{ll} < 50 \text{ GeV}$, *vi*) the missing relative transverse energy satisfies $E_{T,\text{rel}}^{\text{miss}} > 25$ GeV. We note that the missing relative transverse energy is defined as

$$E_{T,\text{rel}}^{\text{miss}} = |\mathbf{p}_T^{\text{miss}}| \sin \Delta\phi_{\min}, \quad (3.1)$$

where $\Delta\phi_{\min} = \min(\Delta\phi_{\text{miss}}, \pi/2)$ and $\Delta\phi_{\text{miss}}$ is the azimuthal angle between the missing transverse momentum vector $\mathbf{p}_T^{\text{miss}}$ and the momentum of the nearest charged lepton or jet with $p_T > 25$ GeV. Jets are identified using the anti- k_\perp algorithm with $R = 0.4$ and $p_{T,j} > 25$ GeV. All jets must have pseudorapidities in the region $|\eta_j| < 4.5$. For the WW process we require additionally that the charged lepton system has a transverse momentum $p_{T,ll} > 30$ GeV.

The cross-sections obtained using these cuts are shown in Table 2. While the importance of NLO QCD corrections is considerably reduced with these cuts, the relative importance of gluon fusion corrections increases by a factor of two, compared to the standard cuts. The change to the *exclusive* NLO cross-sections for $pp \rightarrow W^+W^-$ and $pp \rightarrow W^+W^- + j$ because of the gluon fusion contribution is about 6% for $\sqrt{s} = 8$ TeV and is close to 10% for $\sqrt{s} = 14$ TeV. Therefore, for the Higgs search cuts, gluon fusion corrections are larger than the scale variations of the exclusive NLO QCD cross-sections for the process W^+W^- , and comparable to the scale variations of the exclusive NLO QCD cross-sections for the process $W^+W^- + 1$ jet.

Furthermore, using the Higgs search cuts described above and a Higgs mass of $m_H = 125$ GeV, the *signal* $H \rightarrow WW$ cross-section (in the $e^+\mu^-$ channel considered here) at NLO QCD is approximately 5 fb (12 fb) at 8 TeV (14 TeV) in the 0-jet channel and 2 fb (5 fb) at 8 TeV (14 TeV) in the 1-jet channel. The gluon fusion corrections to the WW background alone therefore amount to almost half of the signal cross-sections.

We note that the gluon fusion corrections to $pp \rightarrow W^+W^-$ that we find in this paper are significantly smaller than $\mathcal{O}(30\%)$ effects reported in Refs. [26, 27]. This happens because the cuts used in those references are more aggressive than the cuts that we use here. In particular, stronger cuts on $\Delta\phi_{ll}$, m_{ll} and, especially, on the transverse momenta of the charged leptons, account for the larger $gg \rightarrow WW$ contribution. We have checked that with cuts similar to those adopted in Ref. [26, 27] we indeed would have a significant increase in the relative importance of the gluon fusion contribution.

Finally, the integrated cross-section – even when computed with cuts optimized for the Higgs boson searches – is not the whole story since experimentalists rely on shapes

³In the measurements of ATLAS [42] the rapidity region $1.37 < |\eta| < 1.52$ is excluded for electrons. For simplicity we use instead full acceptance both for electrons and muons. We also ignore issues related to specifics of the detector. Our treatment of the lepton separation is also slightly simpler than the one in Ref. [42].

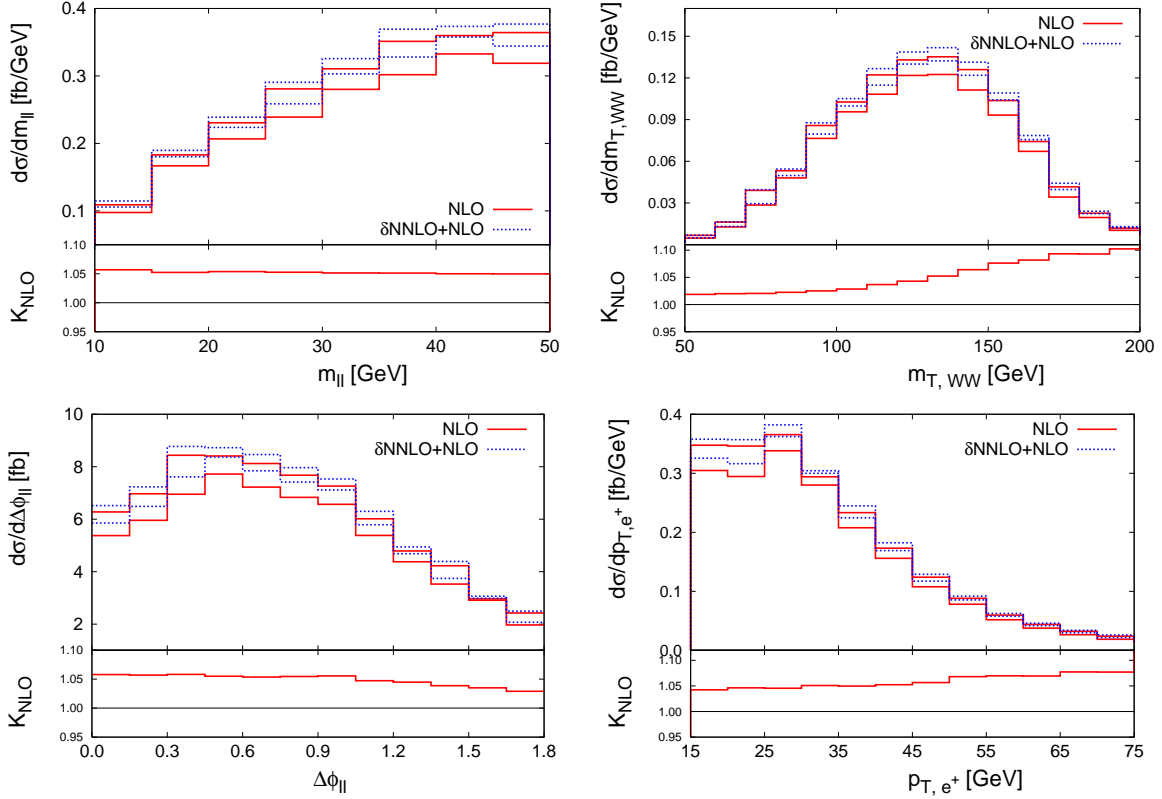


Figure 4: Distributions of the mass of the charged lepton system m_{ll} , transverse mass of the W -pair $m_{T,WW}$, the azimuthal angle between the leptons $\Delta\phi_{ll}$ and the transverse momentum of the positron p_{T,e^+} , shown at NLO accuracy with and without the fermion loop NNLO contribution. We use the Higgs search cuts as described in the text, and we display results for the 8 TeV LHC. The upper and lower bands show the maximum and minimum deviations from the central scale value $2m_W$. The ratio K_{NLO} as defined in Eq.(3.3) is also displayed.

Higgs search cuts

		σ_{LO}	$\sigma_{\text{NLO}}^{\text{incl}}$	$\sigma_{\text{NLO}}^{\text{excl}}$	$\delta\sigma_{\text{NNLO}}$	$\delta\sigma_{\text{NNLO}}/\sigma_{\text{NLO}}^{\text{excl}}$
8 TeV	WW	$35.6(1)^{+0.9}_{-1.3}$	$51.1(1)^{-0.4}_{+0.9}$	$38.8(1)^{+1.0}_{-0.8}$	$2.7(1)^{-0.5}_{+0.7}$	7.0%
	WWj	$12.6(1)^{-1.5}_{+1.8}$	$10.8(1)^{+0.3}_{-0.7}$	$10.6(1)^{+0.3}_{-0.9}$	$0.6(1)^{-0.2}_{+0.2}$	5.7%
14 TeV	WW	$63.4(1)^{+3.9}_{-4.7}$	$91.9(2)^{-0.1}_{+0.4}$	$63.4(2)^{+2.1}_{-2.0}$	$7.5(1)^{-1.2}_{+1.5}$	11.8%
	WWj	$28.7(1)^{-2.6}_{+2.9}$	$21.6(1)^{+1.2}_{-2.1}$	$20.5(1)^{+1.7}_{-2.2}$	$1.8(2)^{-0.5}_{+0.7}$	8.8%

Table 2: As for table 1, but using the ATLAS Higgs search cuts as described in the text. The ratio in the last column is taken using the *exclusive* NLO cross-section.

of distributions to distinguish signal and backgrounds. In Fig. 4 we show the relevant kinematic distributions for the background W^+W^-+j process, paying particular attention to the modifications caused by the gluon fusion contribution. We display distributions in the azimuthal angle between the charged leptons, the invariant mass of the charged leptons,

the transverse momentum of the positron, and the transverse mass of the W^+W^- pair defined as

$$m_{T,WW} = \sqrt{(E_{T,u} + p_{T,\text{miss}})^2 - |\mathbf{p}_{T,\text{miss}} + \mathbf{p}_{T,u}|^2}. \quad (3.2)$$

Here $E_{T,u} = \sqrt{|\mathbf{p}_{T,u}|^2 + m_u^2}$ and $p_{T,\text{miss}} = |\mathbf{p}_{T,\text{miss}}|$. Since spin correlations in $H \rightarrow W^+W^-$ decays force the two charged leptons to be close to each other, the most interesting, signal-rich regions of the $\Delta\phi_{ll}$ - and m_{ll} -distributions are at small values of the corresponding variables. The distribution in the transverse mass of the W^+W^- pair is also useful because restricting this variable to values comparable to the Higgs boson mass removes the interference between the Higgs signal and the background from direct W^+W^- production [43]. Furthermore, ATLAS collaboration uses the distribution of $m_{T,WW}$ to test for the presence of a signal [42]. In the lower panes in Fig. 4, we show the differential K -factors defined as

$$K_{\text{NLO}} = \left. \frac{d\sigma_{\text{NLO}+\delta\text{NNLO}}}{d\sigma_{\text{NLO}}} \right|_{\mu=2m_W}. \quad (3.3)$$

We notice that the K_{NLO} factor spread over the distributions m_{ll} , $\Delta\phi_{ll}$ and p_{T,e^+} is close to uniform, while the relative importance of the $\delta\sigma_{\text{NNLO}}$ contribution increases with $m_{T,WW}$.

4. Conclusion

In this paper, we considered the gluon fusion contribution to the production of a pair of W -bosons and a jet at the LHC. While formally part of the NNLO QCD correction to the $pp \rightarrow W^+W^- + \text{jet}$ process, this contribution can be treated separately because it is finite and gauge invariant. In addition, gluon fusion contributions are enhanced by the large gluon flux at the LHC and may therefore be an important part of the backgrounds to Higgs boson searches. In fact, it was found in Refs. [26,27] that, for a particular set of cuts, the $gg \rightarrow W^+W^-$ contribution becomes the largest radiative correction to $pp \rightarrow W^+W^-$, changing the leading order contribution by as much as 30%.

In the current paper, we used the set of cuts employed by the ATLAS collaboration in their current searches for the Higgs boson to estimate the gluon fusion contribution to $pp \rightarrow W^+W^- + 0$ or 1 jet and we find significantly smaller radiative corrections than the results quoted in Refs. [26,27]. This is a combined effect of looser cuts on $\Delta\phi_{ll}$, m_{ll} and the lepton transverse momenta currently used by the ATLAS collaboration compared to those used for the discussion in Refs. [26,27]. For the ATLAS Higgs search cuts we find that the gluon fusion contribution to $pp \rightarrow W^+W^-j$ is somewhat larger than, but still comparable to, the scale uncertainty of the exclusive NLO cross-section and most of the kinematic distributions. However, as our results show, these conclusions very much depend on the exact cuts applied. Should the experimental cuts change significantly, the calculations reported in this paper should be reconsidered.

Acknowledgments K.M. acknowledges useful conversations with F. Petriello about the importance of gluon fusion background processes for the Higgs boson searches. This research is supported in part by NSF grants PHY-0855365, by the DOE grant DE-AC02-06CD11357, by the LHCPhenoNet network under the Grant Agreement PITN-GA-2010-

	$ A_{f,0} $	$ A_{f,m} $
g_1^+, g_2^+, g_3^+	3.844351	0.9542655
g_1^+, g_2^+, g_3^-	5.699256	1.606166
g_1^+, g_2^-, g_3^-	3.522647	6.204687
g_1^-, g_2^-, g_3^-	23.21330	26.65234

Table 3: Numerical results for the massless and massive fermion loop primitive amplitudes $A_{f,0}(g_1, g_2, g_3)$ and $A_{f,m}(g_1, g_2, g_3)$, in units of 10^{-6}GeV^{-3} .

264564, and by the British Science and Technology Facilities Council. M.S. is grateful for support from the Director’s Fellowship of Argonne National Laboratory.

A. Appendix

In this appendix, we display the results for some of the primitive amplitudes, as well as a full amplitude summed over helicities, for a single phase space point. We consider the process $gg \rightarrow W^+(\rightarrow \nu_e e^+)W^-(\rightarrow \mu^- \bar{\nu}_\mu)g$, and use the phase-space point (E, p_x, p_y, p_z) (in GeV):

$$\begin{aligned}
p_{g_1} &= (-500, 0, 0, -500), \\
p_{g_2} &= (-500, 0, 0, 500), \\
p_{g_3} &= (86.3540681437814, -15.2133893202618, 37.6335512949163, -76.2187226821854), \\
p_{\nu_e} &= (414.130068374543, 232.145564945939, 332.7544367808, -82.9857518524426), \\
p_{e^+} &= (91.8751521026384, -43.3570226791011, -24.0058236140057, 77.3623460793435), \\
p_{\mu^-} &= (280.118181809376, -83.1261116505822, -263.203856758651, 47.7490851160266), \\
p_{\bar{\nu}_\mu} &= (127.522529569661, -90.4490412959935, -83.1783077030789, 34.0930433392580).
\end{aligned} \tag{A.1}$$

We present the results for the primitive amplitude $A_f(g_1, g_2, g_3)$ as defined in Eq. (2.1) for four sets of helicities of the three gluons. In Table 3, we display both massless and massive fermion loop amplitudes as defined in Eq. (2.2). We show only the finite parts of the amplitude, since there are no poles.

We also give results for the full amplitude squared, that is, the color-squared amplitude from Eq. (2.1) summed over all gluon helicities. If we consider only one massless generation in the loop, the result is $8.348897 \times 10^{-8}\text{GeV}^{-6}$. If we consider one massive generation in the loop, the result is $1.128414 \times 10^{-7}\text{GeV}^{-6}$. For the setup used in deriving our results, i.e. two massless and one massive generation in the loop, the amplitude squared is $7.830968 \times 10^{-7}\text{GeV}^{-6}$.

References

- [1] **ATLAS** Collaboration, G. Aad *et al.* *Phys.Lett.* **B710** (2012) 49–66, [[hep-ex/1202.1408](#)].
- [2] **CMS** Collaboration, S. Chatrchyan *et al.* [[hep-ex/1202.1488](#)].
- [3] R. V. Harlander and W. B. Kilgore, *Phys. Rev. Lett.* **88** (2002) 201801, [[hep-ph/0201206](#)].

- [4] C. Anastasiou and K. Melnikov, *Nucl. Phys.* **B646** (2002) 220, [[hep-ph/0207004](#)].
- [5] V. Ravindran, J. Smith and W. L. van Neerven, *Nucl. Phys.* **B665** (2003) 325, [[hep-ph/0302135](#)].
- [6] D. de Florian, M. Grazzini and Z. Kunszt, *Phys. Rev. Lett.* **82** (1999) 5209, [[hep-ph/9902483](#)].
- [7] V. Ravindran, J. Smith and W. L. Van Neerven, *Nucl. Phys.* **B634** (2002) 247, [[hep-ph/0201114](#)].
- [8] C. J. Glosser and C. R. Schmidt, *JHEP* **0212** (2002) 016, [[hep-ph/0209248](#)].
- [9] J. M. Campbell, R. K. Ellis and G. Zanderighi, *JHEP* **0610** (2006) 028, [[hep-ph/0608194](#)].
- [10] J. M. Campbell, R. K. Ellis and C. Williams, *Phys. Rev.* **D81** (2010) 074023, [[hep-ph/1001.4495](#)].
- [11] J. Ohnemus, *Phys.Rev.* **D44** (1991) 1403–1414.
- [12] S. Frixione, *Nucl.Phys.* **B410** (1993) 280–324.
- [13] L. J. Dixon, Z. Kunszt, and A. Signer, *Nucl.Phys.* **B531** (1998) 3–23, [[hep-ph/9803250](#)].
- [14] L. J. Dixon, Z. Kunszt, and A. Signer, *Phys.Rev.* **D60** (1999) 114037, [[hep-ph/9907305](#)].
- [15] J. M. Campbell and R. Ellis *Phys.Rev.*, **D60** (1999) 113006, [[hep-ph/9905386](#)].
- [16] J. M. Campbell, R. K. Ellis, and C. Williams, *JHEP* **1107** (2011) 018, [[hep-ph/1105.0020](#)].
- [17] S. Frixione and B. R. Webber, *JHEP* **0206** (2002) 029, [[hep-ph/0204244](#)].
- [18] T. Melia, P. Nason, R. Rontsch, and G. Zanderighi, *JHEP* **1111** (2011) 078, [[hep-ph/1107.5051](#)].
- [19] J. M. Campbell, R. K. Ellis, and G. Zanderighi, *JHEP* **0712** (2007) 056, [[hep-ph/0710.1832](#)].
- [20] S. Dittmaier, S. Kallweit, and P. Uwer, *Phys.Rev.Lett.* **100** (2008) 062003, [[hep-ph/0710.1577](#)].
- [21] S. Dittmaier, S. Kallweit and P. Uwer, *Nucl. Phys. B* **826** (2010) 18 [[arXiv:0908.4124](#) [[hep-ph](#)]].
- [22] T. Melia, K. Melnikov, R. Rontsch, and G. Zanderighi, *JHEP* **1012** (2010) 053, [[hep-ph/1007.5313](#)].
- [23] T. Melia, K. Melnikov, R. Rontsch, and G. Zanderighi, *Phys.Rev.* **D83** (2011) 114043, [[hep-ph/1104.2327](#)].
- [24] N. Greiner, G. Heinrich, P. Mastrolia, G. Ossola, T. Reiter, *et. al.* [[hep-ph/1202.6004](#)].
- [25] C. Kao and D. A. Dicus, *Phys.Rev.* **D43** (1991) 1555–1559.
- [26] T. Binoth, M. Ciccolini, N. Kauer, and M. Kramer, *JHEP* **0503** (2005) 065, [[hep-ph/0503094](#)].
- [27] T. Binoth, M. Ciccolini, N. Kauer, and M. Kramer, *JHEP* **0612** (2006) 046, [[hep-ph/0611170](#)].
- [28] R. K. Ellis, W. Giele, and Z. Kunszt, *JHEP* **0803** (2008) 003, [[hep-ph/0708.2398](#)].
- [29] W. T. Giele, Z. Kunszt, and K. Melnikov, *JHEP* **0804** (2008) 049, [[hep-ph/0801.2237](#)].

- [30] R. K. Ellis, W. T. Giele, Z. Kunszt, and K. Melnikov, *Nucl.Phys.* **B822** (2009) 270–282, [[hep-ph/0806.3467](#)].
- [31] R. K. Ellis, Z. Kunszt, K. Melnikov, and G. Zanderighi, [[hep-ph/1105.4319](#)].
- [32] G. Ossola, C. G. Papadopoulos, and R. Pittau, *Nucl.Phys.* **B763** (2007) 147–169, [[hep-ph/0609007](#)].
- [33] J. A. Maestre, S. Alioli, J. R. Andersen, R. D. Ball, A. Buckley, M. Cacciari, F. Campanario and N. Chanon *et al.*, [arXiv:1203.6803](#) [[hep-ph](#)].
- [34] V. Hirschi, R. Frederix, S. Frixione, M. V. Garzelli, F. Maltoni and R. Pittau, *JHEP* **1105** (2011) 044, [[hep-ph/1103.0621](#)].
- [35] G. Bevilacqua, M. Czakon, M. Garzelli, A. van Hameren, A. Kardos, *et. al.*, [[hep-ph/1110.1499](#)].
- [36] G. Cullen, N. Greiner, G. Heinrich, G. Luisoni, P. Mastrolia, *et. al.*, [[hep-ph/1201.2782](#)].
- [37] F. Cascioli, P. Maierhofer and S. Pozzorini, *Phys. Rev. Lett.* **108** (2012) 111601 [[arXiv:1111.5206](#) [[hep-ph](#)]].
- [38] F. A. Berends and W. Giele, *Phys. Lett.* **B232** (1989) 266.
- [39] M. Cacciari, G. P. Salam, and G. Soyez, *JHEP* **04** (2008) 063, [[hep-ph/0802.1189](#)].
- [40] M. Cacciari, G. P. Salam, and G. Soyez, *Eur.Phys.J.* **C72** (2012) 1896, [[hep-ph/1111.6097](#)].
- [41] A. D. Martin, W. J. Stirling, R. S. Thorne and G. Watt, *Eur. Phys. J.* **C63** (2009) 189, [[hep-ph/0901.0002](#)].
- [42] **ATLAS** Collaboration, ATLAS-CONF-2012-12 (2012).
- [43] J. M. Campbell, R. K. Ellis, and C. Williams, *JHEP* **1110** (2011) 005, [[hep-ph/1107.5569](#)].